Journal of Molecular Spectroscopy 274 (2012) 22–27

Contents lists available at SciVerse ScienceDirect

Journal of Molecular Spectroscopy

journal homepage: www.elsevier.com/locate/jms

Fourier transform emission spectroscopy of the $A^2\Pi$–$X^2\Sigma^+$ (red) system of $^{13}C^{14}N$ (II)

R.S. Ram [a,b,*], P.F. Bernath [a,c]

[a] Department of Chemistry, University of York, Heslington, York YO10 5DD, UK
[b] Department of Chemistry, University of Arizona, Tucson, AZ 85721, USA
[c] Department of Chemistry and Biochemistry, Old Dominion University, Norfolk, VA 23529, USA

ARTICLE INFO

Article history:
Received 6 March 2012
In revised form 21 March 2012
Available online 3 April 2012

Keywords:
Electronic spectra
Rotational analysis
Free radicals
Solar spectra
Carbon stars

ABSTRACT

High resolution emission spectra of the $A^2\Pi$–$X^2\Sigma^+$ transition of $^{13}C^{14}N$ have been measured in the 15 000–24 000 cm^{-1} region. Molecules were produced by the reaction of $^{13}CH_4$ and $^{14}N_2$ in an active nitrogen afterglow discharge. The spectra were recorded using the Fourier transform spectrometer associated with the McMath-Pierce Solar Telescope of the National Solar Observatory. A rotational analysis of 27 bands involving the excited state vibrational levels v' = 9–22 and the ground state vibrational levels up to v'' = 12 has been obtained. An improved set of spectroscopic constants has been determined for the v = 0–22 levels of the $A^2\Pi$ state by combining the present measurements with those reported previously for the v = 0–8 vibrational levels of the $A^2\Pi$ state [Ram et al., Astrophys. J. Suppl. Ser. 188 (2010) 500] and existing infrared and millimeter-wave measurements of $^{13}C^{14}N$. The 6–3, 7–4, 8–5 and 9–6 bands of the $B^2\Sigma^+$–$A^2\Pi$ transition were also identified in the 23 300–24 000 cm^{-1} region and were included in the final analysis. An experimental line list and calculated term values are provided.

1. Introduction

Electronic spectra of CN are known for more than a century through characteristic bands present in the visible and ultraviolet regions. These bands belong to the $A^2\Pi$–$X^2\Sigma^+$ (red) and $B^2\Sigma^+$–$X^2\Sigma^+$ (violet) transitions which extend from the near infrared to the ultraviolet regions and are very persistent. This radical is frequently observed in a wide variety of sources such as arcs, electrical discharges, flames and shock tubes and its spectra now extend from the microwave to the vacuum ultraviolet [1].

This radical has been found in a wide range of astronomical sources such as comets [2–5] stars [6,7], the sun [8], circumstellar shells [9,10], interstellar clouds [11,12] and the integrated light of galaxies [13]. The CN lines of the violet system were also identified in the spectra of the Red Rectangle nebula [HD 44179] [14]. The presence of CN in astronomical objects makes it a key species to probe carbon and nitrogen abundances, as well as C and N isotopic ratios. The carbon and nitrogen isotopic abundance ratios give information on nucleosynthesis and chemical evolution in galaxies [15]. Millimeter wave surveys of ^{12}CN and ^{13}CN in dark molecular clouds have shown a Galactic abundance gradient attributed to chemical evolution [16,17] and also shed light on star formation in galaxies [13].

The $A^2\Pi$–$X^2\Sigma^+$ (red) and $B^2\Sigma^+$–$X^2\Sigma^+$ (violet) transitions of CN, in particular, have been extensively studied because of their astrophysical importance. The previous studies of $^{12}C^{14}N$ have been summarized in some recent papers on the red [18,19] and violet [19–21] systems of $^{12}C^{14}N$ and references to the previous studies on $^{13}C^{14}N$ can be found in the recent papers on the red [23] and violet [24] systems of $^{13}C^{14}N$. Recently, the high resolution spectra of these two transitions of the $^{12}C^{15}N$ isotopologue have been studied by Colin and Bernath [25]. Because of the astrophysical importance of CN, Fay and Wyller [26] have stressed on the need for high resolution measurements of the $^{13}C^{14}N$ red system bands near 1 μm and longer wavelengths. A line list commonly used in current astronomical work is that of Plez, as discussed in Hill et al. [27]. This list is drawn from eight separate sources and is inadequate for $^{13}C^{14}N$ as has been pointed out by Garcia-Hernandez et al. [28]. There is, therefore, a need for high resolution measurements of CN and its isotopologues to improve the simulation of astronomical spectra and obtain more accurate $^{12}C/^{13}C$ abundance ratios.

Hempel et al. [29] have measured the fundamental 1–0 band of $^{12}C^{14}N$ and $^{13}C^{14}N$, and Hübner et al. [30] have reported the measurements of fundamental bands of $^{12}C^{14}N$, $^{13}C^{14}N$, $^{12}C^{15}N$, $^{13}C^{15}N$ isotopologues using tunable diode laser absorption spectroscopy. The millimeter wave studies of the $X^2\Sigma^+$ ground state of $^{13}C^{14}N$ were obtained by Bogey et al. [31,32] and pure rotational

* Corresponding author at: Department of Chemistry, University of York, Heslington, York YO10 5DD, UK. Fax: +44 0 1904 432516.
E-mail address: rr662@york.ac.uk (R.S. Ram).

0022-2852/$ - see front matter © 2012 Elsevier Inc. All rights reserved.
http://dx.doi.org/10.1016/j.jms.2012.03.008

measurements were reported for the $v = 0–9$ vibrational levels of the ground state [32].

Jørgensen and Larsson [33] have calculated the molecular opacities for the CN, $A^2\Pi–X^2\Sigma^+$ transition at temperatures ranging from 1000 K to 6000 K and rotational lines were calculated for the $^{12}C^{14}N$, $^{13}C^{14}N$, $^{12}C^{15}N$, $^{13}C^{15}N$ isotopologues for transitions between vibrational levels $v = 0–30$ of the ground and excited states using available and extrapolated spectroscopic constants. In a recent theoretical study, Shi et al. [34] investigated the potential energy curves of the $A^2\Pi$ and $X^2\Sigma^+$ states using high level ab initio calculations and estimated spectroscopic parameters for the four isotopic species $^{12}C^{14}N$, $^{13}C^{14}N$, $^{12}C^{15}N$ and $^{13}C^{15}N$.

Recently we have reported on extensive high resolution studies of the red and violet transitions of $^{12}C^{14}N$ [21,22] and $^{13}C^{14}N$ [23,24] with the aim of providing an accurate line list for the bands, and improved spectroscopic constants and term values for the $A^2\Pi$ and $B^2\Sigma^+$ states of the two isotopologues. For $^{12}C^{14}N$ we have reported term values and spectroscopic constants for the $v = 0–22$ vibrational levels of the $A^2\Pi$ state [21] and $v = 0–15$ vibrational level of the $B^2\Sigma^+$ and $X^2\Sigma^+$ states [22] from the rotational analysis of a large number of bands. In the case of $^{13}C^{14}N$, we have recently reported on the rotational analysis of 22 bands of the $A^2\Pi–X^2\Sigma^+$ transition involving the $v'' = 0–5$ and $v' = 0–8$ vibrational levels [23] while for the violet system we obtained a rotational analysis of 52 bands involving vibrational levels up to $v = 15$ of the $B^2\Sigma^+$ and $X^2\Sigma^+$ states [24]. These studies have provided an extensive set of spectroscopic constants and rotational line positions that were used to show that many unidentified lines in the near infrared spectra of carbon stars were due to $^{13}C^{14}N$ [23].

At the time of our previous study of the $A^2\Pi–X^2\Sigma^+$ transition of $^{13}C^{14}N$ [23], we noted the presence of a large number of bands in the 15000–24000 cm^{-1} region which were left unassigned because of their relatively weak intensity and overlapping. After the rotational analysis of these bands, we have extended the red system of $^{13}C^{14}N$ to much higher vibrational levels of the $A^2\Pi$ state. Several violet degraded bands present in the 23300–24000 cm^{-1} region have been identified as belonging to the $B^2\Sigma^+–A^2\Pi$ transition of $^{13}C^{14}N$, observed for the first time. In this paper we report on the rotational analysis of 27 bands of the $A^2\Pi–X^2\Sigma^+$ transition involving vibrational levels $v = 9–22$ of the $A^2\Pi$ state and the 6–3, 7–4, 8–5 and 9–6 bands of the $B^2\Sigma^+–A^2\Pi$ transition of $^{13}C^{14}N$. In the final fit we have combined our new measurements with our previous measurements of the $A^2\Pi–X^2\Sigma^+$ bands in the 4000–15000 cm^{-1} region [23], the measurements of the $B^2\Sigma^+–X^2\Sigma^+$ bands [24], all red and infrared measurements [29,30] and previous millimeter-wave measurements [31,32] with the aim of providing an accurate line list for all bands, and improved spectroscopic constants and term values for the $v = 0–22$ vibrational levels of the $A^2\Pi$ state.

2. Experimental

The spectra of $^{13}C^{14}N$ used in the present analysis were recorded by J. Brault (deceased) and R. Engleman in 1992 using the Fourier transform spectrometer associated with McMath-Pierce Solar Telescope of the National Solar Observatory located at Kitt Peak. The molecules were produced in a lamp by adding mixture of argon and a trace of $^{13}CH_4$ to active nitrogen, $^{14}N_2$, made in a microwave discharge. Spectra in the 2900–31000 cm^{-1} region were recorded in two parts. The 2900–16000 cm^{-1} region was recorded using the CaF_2 beamsplitter, InSb detectors, and RG610 filters while the other 9000–31000 cm^{-1} region was recorded using the UV beam splitter and midrange Si photodiode detectors. The spectra in the two regions were recorded at the respective resolution of 0.016 cm^{-1} and 0.03 cm^{-1} by co-adding 5 and 4 scans, respectively.

The spectra recorded with the active nitrogen source were free from any $^{12}C^{14}N$ impurity. The line positions were extracted from the observed spectra using a data reduction program called PC-DECOMP developed by J. Brault. The peak positions were determined by fitting a Voigt line shape function to each spectral feature. The spectra in the 15000–24000 cm^{-1} region were calibrated by transferring calibration from the $B^2\Sigma^+–X^2\Sigma^+$ bands, since this region of the $A^2\Pi–X^2\Sigma^+$ system is free from any atomic or molecular features suitable for independent calibration. The $B^2\Sigma^+–X^2\Sigma^+$ bands were calibrated using the Ar line measurements by Whaling et al. [35] as corrected by Sansonetti [36]. The precision of measurement is expected to be better than ±0.002 cm^{-1} for the stronger and unblended lines. However the lower J rotational lines in some branches were blended because of the partially-resolved splitting of the main and satellite branches; the blended and weaker lines have uncertainty of ±0.005 cm^{-1} or higher.

3. Observations

As was noted in the case of the red system of $^{12}C^{14}N$, the spectra recorded using the active nitrogen afterglow discharge have a low rotational temperature (~300 K) and high vibrational temperatures. This results in the observation of vibrational bands with higher v's than other sources including a regular microwave discharge, high temperature furnaces and arc sources. In fact we have been able to observe bands with vibrational levels up to $v' = 22$ of the $A^2\Pi$ state and $v'' = 12$ of the $X^2\Sigma^+$ state from the afterglow spectra. Because of low rotational temperatures the rotational lines in different bands were typically observed to J values < 30.5 even in the strongest bands.

A few bands located in the 23300–24000 cm^{-1} region have been identified belonging to the $B^2\Sigma^+–A^2\Pi$ transition while the $A^2\Pi–X^2\Sigma^+$ (red) and $B^2\Sigma^+–X^2\Sigma^+$ (violet) bands are located in the 3500–22500 cm^{-1} and 20000–30000 cm^{-1} regions, respectively. Except for the lower sequence bands, the spectra of the red and violet transitions appear complex because of overlapping of the different sequence bands as well as an irregular intensity pattern in the different sequence bands. The irregular intensity pattern of higher vibrational bands arises because of interactions in the excited state, making it difficult to make any vibrational assignments without a proper rotational analysis. Therefore, most of the bands with reasonable intensity were measured and rotationally analyzed in order to make a vibrational assignment. In total 27 bands with $v' = 9–22$ excited state vibrational levels were rotationally analyzed. All these bands belong to vibrational sequences ranging from $\Delta v = 5$ to $\Delta v = 11$.

Each band of a $^2\Pi–^2\Sigma^+$ transition consists of two sub-bands, $^2\Pi_{1/2}–^2\Sigma^+$ and $^2\Pi_{3/2}–^2\Sigma^+$ because the $A^2\Pi$ state belongs to Hund's coupling case (a). Since the $A^2\Pi$ state of $^{13}C^{14}N$ is inverted, the $^2\Pi_{3/2}$ component lies below the $^2\Pi_{1/2}$ component. Following the traditional convention these two components are labeled as F_1 and F_2, respectively. With the selection rule $\Delta J = 0, \pm1$, each sub-band consists of three main and three satellite branches depending on whether the $X^2\Sigma^+$ levels are F_1 or F_2. Therefore, the $^2\Pi_{3/2}–^2\Sigma^+$ sub-band consists of P_{11}, Q_{11}, R_{11}, P_{12}, Q_{12} and R_{12} branches and the $^2\Pi_{1/2}–^2\Sigma^+$ sub-band consists of P_{22}, Q_{22}, R_{22}, P_{21}, Q_{21} and R_{21} branches. An illustrative energy level diagram of a $^2\Pi_i–^2\Sigma^+$ transition can be found in a paper, for example, on the Comet-tail system of CO^+ [37]. This method of labeling the branches has been adopted in the previous studies of the $A^2\Pi_i–X^2\Sigma^+$ transition of $^{12}C^{14}N$ [38] and $^{13}C^{14}N$ [39]. Some of the satellite branches are much weaker than the main branches and have not been identified in some bands due to weak intensity and unresolved splitting from the main branches. A description of the assigned bands is provided in the following sections.

3.1. The $\Delta v = 5, 6, 7, 8$ sequences

We have measured the rotational lines belonging to 9–4, 10–5 and 11–6 bands belonging to the $\Delta v = 5$ sequence; 9–3, 10–4, 13–7 and 14–8 bands of the $\Delta v = 6$ sequence; 12–5, 14–7, 15–8,16–9 and 18–11 bands of the $\Delta v = 7$ sequence and 14–6, 15–7, 16–8, 17–9, 18–10 and 19–11 bands of the $\Delta v = 8$ sequence. These bands are relatively strong in intensity compared to other bands of these sequences because of favorable Franck–Condon factors or intensity enhancement from interactions in the excited state. We have obtained a rotational analysis of all these bands by comparing their lower state combination differences with the corresponding values obtained from the previous analysis of the $B^2\Sigma^+$–$X^2\Sigma^+$ transition [24]. We have also noticed that the intensity of bands in the higher Δv sequences peaks for relatively high v values and then slowly decreases with v, as observed in the case of $^{12}C^{14}N$ [21].

3.2. The $\Delta v = 9$, 10 and 11 sequences

We have obtained the rotational analysis of the 18–9, 19–10, 20–11and 21–12 bands of the $\Delta v = 9$ sequence; 19–9, 21–11 and 22–12 bands of the $\Delta v = 10$ sequence and 21–10, and 22–11 bands of the $\Delta v = 11$ sequence. A part of the 21–11 band showing some low J lines in the head-forming branches of the $A^2\Pi_{1/2}$–$X^2\Sigma^+$ sub-band has been provided in Fig. 1. As can be seen, the R_2 and Q_{21} branches which overlap at lower N values, gradually split for higher N values.

3.3. The 6–3, 7–4, 8–5 and 9–6 bands of the $B^2\Sigma^+$–$A^2\Pi$ transition

Several violet degraded bands were weakly present in our spectra in the 23300–24000 cm^{-1} region. After a rotational analysis these bands were identified belonging to the $B^2\Sigma^+$–$A^2\Pi$ transition of $^{13}C^{14}N$. This type of transition was first observed for $^{12}C^{14}N$ by LeBlanc [40] in 1967 from the reaction of the active nitrogen with $^{12}CH_4$ and later by Conley et al. [41] and Furio et al. [42] by laser excitation spectroscopy. Four $^{13}C^{14}N$ bands with lower wavenumber P heads at 23322, 23457, 23562 and 23635 cm^{-1} were assigned as the 6–3, 7–4, 8–5 and 9–6 bands of the $B^2\Sigma^+$–$A^2\Pi$ transition. Bands belonging to this transition are much weaker in intensity than the bands in the red and violet systems and only the main branches could be identified. Rotational assignment in these bands was made by comparing the combination differences from these bands with those from the common vibrational levels of the $A^2\Pi$–$X^2\Sigma^+$ [23] and the $B^2\Sigma^+$–$X^2\Sigma^+$ [24] transitions. The rotational lines of the $B^2\Sigma^+$–$A^2\Pi$ bands have relatively larger uncertainty because of much weaker intensity than the other two transitions and were given lower weights than the bands of the $A^2\Pi$–$X^2\Sigma^+$ and $B^2\Sigma^+$–$X^2\Sigma^+$ transitions.

4. Analysis and discussion

The rotational constants of the different vibrational levels were determined by fitting the measured wavenumbers of rotational lines of different bands with the effective N^2 Hamiltonian of Brown et al. [43]. The matrix elements of this Hamiltonian for $^2\Sigma^+$ states are provided, for example, by Douay et al. [44] and those for $^2\Pi$ states are provided by Amiot et al. [45]. The lines in each vibrational band were initially fitted separately using a non-linear least-squares procedure. In the final fit we included the measurements of bands with vibrational levels $v = 0$–8 of the $A^2\Pi$ state reported in a previous publication [23] and the measurements of the $B^2\Sigma^+$–$X^2\Sigma^+$ bands [24]. We have also included the available infrared vibration–rotation measurements by Hempel et al. [29] and Hübner et al. [30], and millimeter wave measurements of Bogey et al. [31,32]. The previous diode laser measurements of the 1–0 fundamental band [29,30] were given lower weights than those quoted in these papers since the reported rotational line positions were the average of the two spin doublets, although the splitting was partly resolved for many lines. The microwave measurements were given weights based on quoted errors for transitions frequencies in the papers by Bogey et al. [31,32], except for a few blended lines. The weights for the weaker and blended lines of the red system were chosen based on the signal-to-noise ratio and extent of blending. The inclusion of the infrared measurements with the current measurements improves the molecular constants for the $A^2\Pi$ state. The rotational lines of the $B^2\Sigma^+$–$A^2\Pi$ bands were also included with suitable weights. Some of the spectroscopic constants of the $X^2\Sigma^+$, $A^2\Pi$ and $B^2\Sigma^+$ states have slightly been modified compared to the values reported previously [23,24] but the changes lie

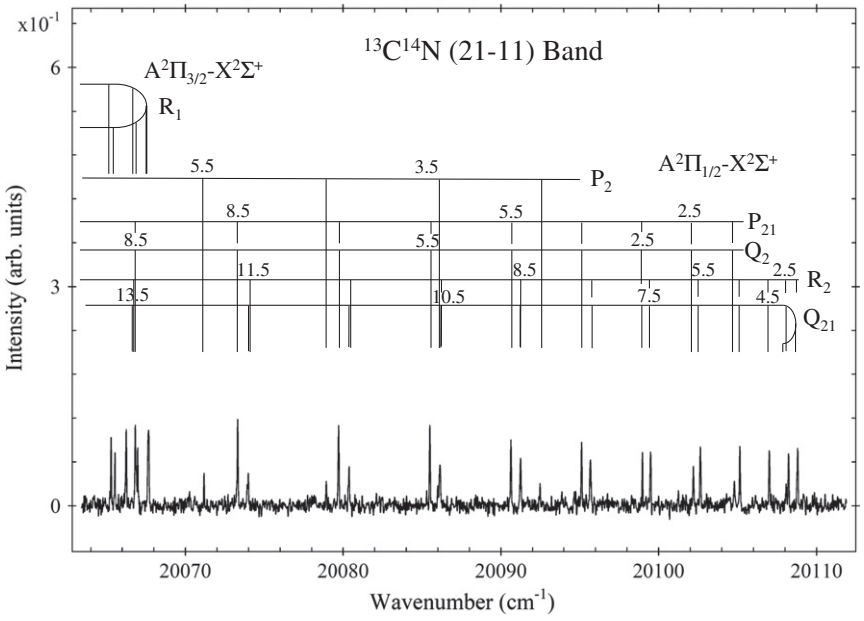

Fig. 1. A part of the spectrum of 21–11 band of the $A^2\Pi_{1/2}$–$X^2\Sigma^+$ sub-band of $^{13}C^{14}N$ near the band heads.

Table 1
Spectroscopic constants (in cm^{-1}) for the $A^2\Pi$ state of $^{13}C^{14}N$.

Constants	$v = 0$	$v = 1$	$v = 2$	$v = 3$	$v = 4$	$v = 5$
T_v	9118.238641(48)	10868.954190(54)	12595.157043(61)	14296.841734(68)	15973.993970(99)	17626.60540(15)
A_v	−52.655413(95)	−52.58401(10)	−52.51016(12)	−52.43419(16)	−52.35571(23)	−52.27962(34)
$A_{Dv} \times 10^4$	−2.0097(28)	−1.9983(29)	−1.9671(34)	−1.9323(53)	−1.9572(98)	−1.905(18)
$A_{Hv} \times 10^8$	0.4737(41)	0.5378(42)	0.6104(56)	0.755(12)	1.185(23)	1.802(58)
B_v	1.63639762(12)	1.62018706(13)	1.60393531(17)	1.58763390(15)	1.57129018(26)	1.55490792(58)
$D_v \times 10^6$	5.636209(92)	5.645719(96)	5.65744(12)	5.665768(55)	5.67928(11)	5.69566(33)
$H_v \times 10^{12}$	1.628(13)	1.233(13)	1.035(18)	–	–	–
$q_v \times 10^4$	−3.5963(11)	−3.6668(11)	−3.7466(13)	−3.8199(22)	−3.9261(49)	−3.985(11)
$q_{Dv} \times 10^8$	0.9673(30)	1.0263(30)	1.1049(40)	1.1345(97)	1.280(21)	1.222(67)
$p_v \times 10^3$	8.0979(54)	8.0595(59)	8.0657(67)	8.0146(98)	8.002(20)	7.923(33)
$p_{Dv} \times 10^7$	−2.722(20)	−2.861(22)	−3.271(29)	−3.445(62)	−4.12(12)	−5.24(28)
	$v = 6$	$v = 7$	$v = 8$	$v = 9$	$v = 10$	$v = 11$
T_v	19254.66292(24)	20858.15240(18)	22437.09704(28)	23988.5682(20)	25520.41253(68)	27025.2611(12)
A_v	−52.21242(52)	−52.16548(37)	−52.25863(54)	−46.6898(41)	−51.2189(14)	−51.2568(15)
$A_{Dv} \times 10^2$	−0.01792(68)	−0.01942(43)	0.01150(95)	2.926(13)	−0.0493(22)	−0.0348(11)
$A_{Hv} \times 10^6$	0.0507(86)	0.1497(46)	0.258(13)	–	0.155(33)	–
B_v	1.5384619(26)	1.5219892(17)	1.5056222(45)	1.477061(72)	1.4721124(97)	1.455180(26)
$D_v \times 10^5$	0.57093(62)	0.57124(34)	0.5523(14)	−1.171(20)	0.5724(27)	0.488(15)
$H_v \times 10^8$	–	–	–	−1.263(27)	–	−0.194(23)
$q_v \times 10^2$	−0.04204(20)	−0.04388(10)	−0.0870(14)	1.5949(51)	−0.04322(67)	−0.0494(11)
$q_{Dv} \times 10^6$	–	–	1.061(37)	−7.124(68)	–	–
p_v	0.007736(39)	0.007800(22)	0.013471(98)	1.1366(28)	0.02646(19)	0.01789(28)
$p_{Dv} \times 10^4$	–	–	–	−3.924(19)	−0.1102(89)	−0.063(14)
	$v = 12$	$v = 13$	$v = 14$	$v = 15$	$v = 16$	$v = 17$
T_v	28505.2401(40)	29960.3303(20)	31390.41170(64)	32795.41713(61)	34175.20600(75)	35529.6090(13)
A_v	−51.1495(72)	−51.0439(40)	−50.8536(12)	−50.6639(11)	−50.4542(14)	−50.2077(26)
$A_{Dv} \times 10^4$	−6.9(29)	−4.99(97)	−3.40(15)	−3.50(14)	−3.38(22)	−3.62(41)
$A_{Hv} \times 10^6$	0.48(18)	−1.59(26)	0.068(18)	0.118(16)	0.492(31)	−0.141(66)
B_v	1.43843(13)	1.421055(47)	1.4043485(64)	1.3872068(60)	1.3699500(94)	1.352268(18)
$D_v \times 10^6$	5.73(20)	2.84(29)	5.852(15)	5.936(14)	5.529(25)	5.534(54)
$H_v \times 10^9$	–	−2.09(32)	–	–	–	–
$q_v \times 10^3$	−0.430(72)	−1.388(50)	−0.6058(43)	−0.589(12)	−0.3648(68)	−1.041(37)
$q_{Dv} \times 10^6$	–	2.26(20)	–	0.103(35)	–	1.05(14)
$p_v \times 10^2$	1.54(58)	1.041(57)	1.525(14)	1.434(16)	0.925(11)	1.984(22)
$p_{Dv} \times 10^5$	–	3.23(50)	−0.166(54)	−0.358(61)	–	–

	$v = 18$	$v = 19$	$v = 20$	$v = 21$	$v = 22$
T_v	36858.48094(66)	38161.62652(78)	39438.4760(56)	40689.43188(85)	41913.64216(98)
A_v	−49.9701(10)	−49.7651(12)	−48.994(12)	−48.9264(11)	−48.5562(17)
$A_{Dv} \times 10^4$	−3.34(13)	−4.41(22)	–	−2.683(62)	−4.21(38)
$A_{Hv} \times 10^7$	1.51(16)	8.64(38)	–	–	6.83(75)
B_v	1.3348494(60)	1.317108(11)	1.297869(28)	1.2807847(89)	1.262536(16)
$D_v \times 10^6$	6.047(13)	5.218(37)	3.709(96)	6.065(20)	6.448(60)
$q_v \times 10^3$	−0.689(12)	0.296(25)	−2.281(49)	−0.858(13)	−0.616(23)
$q_{Dv} \times 10^6$	0.110(32)	1.14(11)	4.27(20)	0.302(31)	0.539(72)
$p_v \times 10^1$	0.1462(16)	0.0890(25)	1.134(34)	0.2130(22)	0.1220(18)
$p_{Dv} \times 10^4$	−0.0257(56)	−0.463(16)	−1.44(11)	−0.0790(70)	–

Note: Numbers quoted in parentheses are one standard deviation error in the last digits.

within the experimental error limits. From this analysis we were able to derive a set of spectroscopic constants for the $v = 0$–22 vibrational levels of the $A^2\Pi$ state.

The spectroscopic constants for the $A^2\Pi$ and $X^2\Sigma^+$ states of $^{13}C^{14}N$ obtained in this fit are provided in Tables 1 and 2, respectively. The spectroscopic parameters T_v (except $v = 0$), B_v, D_v, H_v and γ_v were determined in the $X^2\Sigma^+$ ground state. The spectroscopic parameters T_v, A_v, A_{Dv}, A_{Hv} B_v, D_v, H_v, q_v, q_{Dv}, p_v and p_{Dv} were determined in the $A^2\Pi$ state. A list of measurements used in the determination of the spectroscopic constants along with the obs.-calc. residuals is available as Supplement 1 on ScienceDirect and as part of the Ohio State University Molecular Spectroscopy Archives (http://msa.lib.ohio-state.edu/jmsa_hp.htm). The term values for the observed vibrational levels of the $X^2\Sigma^+$, $A^2\Pi$ and $B^2\Sigma^+$ states calculated using the spectroscopic constants obtained in the final fit (Tables 1 and 2) are provided in Supplement 2. The term values for different vibrational levels have been extrapolated to an additional 20–25 J's higher than those observed in the spectra. The extrapolated term values will have higher uncertainty than the values for the observed levels.

The spectroscopic constants of the different vibrational levels of the $A^2\Pi$ and $X^2\Sigma^+$ states (Tables 1 and 2) have been used to evaluate equilibrium constants for the $A^2\Pi$ and $X^2\Sigma^+$ states of $^{13}C^{14}N$ using the usual expressions [23]. Although the lower vibrational levels of the ground state are relatively free from local perturbations, the term values of the $v = 10$, 11 and 12 levels were given lower weights. During the analysis of the $B^2\Sigma^+$–$X^2\Sigma^+$ transition [24], we observed a strong perturbation in the $v = 13$ vibrational level of the ground state and were unable to obtain the rotational analysis of any B–X bands involving this lower state vibrational level. The effect of interactions were also seen in bands with $v'' = 12$. For the $A^2\Pi$–$X^2\Sigma^+$ transition, our observations are restricted to $v'' = 0$–12 vibrational levels of the ground state. The ground state rotational constants are less affected by perturbations and the ground state equilibrium rotational constants were obtained using rotational constants of all vibrational levels of the ground state.

Table 2
Spectroscopic constants (in cm^{-1}) for the $X^2\Sigma^+$ state of $^{13}C^{14}N$.

Constants	$v = 0$	$v = 1$	$v = 2$	$v = 3$	$v = 4$	$v = 5$	$v = 6$
T_v	0.0	2000.085149(42)	3974.971257(44)	5924.620803(64)	7848.994889(89)	9748.05473(16)	11621.76177(37)
B_v	1.812691744(27)	1.796343167(28)	1.779944756(28)	1.763494605(28)	1.746990597(28)	1.730430474(28)	1.713811608(38)
$D_v \times 10^6$	5.876718(72)	5.885166(74)	5.893939(95)	5.90561(21)	5.91203(24)	5.92570(55)	5.9327(33)
$H_v \times 10^{12}$	3.530(11)	3.382(11)	3.118(20)	3.448(92)	–	–	–
$\gamma_v \times 10^3$	6.95454(19)	6.87872(19)	6.79448(19)	6.70004(19)	6.59137(19)	6.46271(19)	6.30635(19)
	$v = 7$	$v = 8$	$v = 9$	$v = 10$	$v = 11$	$v = 12$	$v = 13$
T_v	13470.07384(38)	15292.94401(38)	17090.32410(45)	18862.16082(58)	20608.38216(60)	22328.82645(74)	–
B_v	1.697131426(34)	1.680386763(34)	1.663574505(35)	1.6466892(39)	1.6296769(59)	1.6123483(95)	–
$D_v \times 10^6$	5.9557(26)	5.9711(26)	5.9925(28)	6.0292(64)	6.037(14)	6.379(26)	–
$\gamma_v \times 10^3$	6.11298(19)	5.87130(19)	5.56824(19)	5.343(32)	5.082(34)	6.554(62)	–

Note: Numbers quoted in parentheses are one standard deviation error in the last digits.

Table 3
Equilibrium constants (in cm^{-1}) for the $A^2\Pi$ state of $^{13}C^{14}N$.

Constants	$A^2\Pi$
T_e	9243.17477(71)
ω_e	1775.21504(69)
$\omega_e x_e$	12.24736(27)
$\omega_e y_e$	−0.001734(29)
B_e	1.6444919(21)
$\alpha_1 \times 10^2$	−1.61781(24)
$\alpha_2 \times 10^5$	−1.657(66)
$\alpha_3 \times 10^7$	6.78(38)
r_e (Å)	1.23303836(79)

Note: Values in parentheses are one standard deviation uncertainties in the last digits.

Table 4
Equilibrium constants (in cm^{-1}) for the $X^2\Sigma^+$ state of $^{13}C^{14}N$.

Constants	$X^2\Sigma^+$
T_e	0.0
ω_e	2025.2509(11)
$\omega_e x_e$	12.57330(57)
$\omega_e y_e$	−0.00572(11)
$\omega_e z_e$	−0.0000530(65)
B_e	1.82084919(48)
$\alpha_1 \times 10^2$	−1.630281(44)
$\alpha_2 \times 10^5$	−2.259(11)
$\alpha_3 \times 10^7$	−4.185(73)
r_e (Å)	1.17180533(16)

Note: Values in parentheses are one standard deviation uncertainties in the last digits.

It can be noticed from Table 1 that most of the higher vibrational levels of the $A^2\Pi$ state, except a few lower levels ($v < 6$) are affected by interactions. The effect of interactions can clearly be noted from the spin–orbit splitting constants of excited state vibrational levels. For example, the A_v values for the $v = 6$, 7, 8, 9 and 10 vibrational levels of the $A^2\Pi$ state are −52.2124, −52.1655, −52.2586, −46.6898 and 51.2189 cm^{-1}, respectively. A large decrease in the value of A_9 to −46.6898 cm^{-1} from $A_8 = -52.2586$ cm^{-1} is an indication of strong interaction of the $v = 9$ vibrational level. A similar observation was made for the $A^2\Pi$ state of $^{12}C^{14}N$ where this effect was noticed for the $v = 8$ vibrational level [21]. These interactions are caused by the close-lying levels of states such as the $B^2\Sigma^+$ state or the higher vibrational levels of the $X^2\Sigma^+$ state. A careful inspection of the term values of the $A^2\Pi$ state and those of the $X^2\Sigma^+$ and $B^2\Sigma^+$ states [24] indicates that the $v' = 9$ vibrational level of the $A^2\Pi$ state interacts strongly with the $v'' = 13$ vibrational level of the $X^2\Sigma^+$ state. Because of interactions, the e-parity levels of the $A^2\Pi_{1/2}$ sub-state are completely misplaced and the Q_{22} branches of the 9–3 and 9–4 bands have to be entirely de-weighted. We have also noted that the $v' = 13$ of the $A^2\Pi$ state interacts with the $v = 2$ vibrational level of the $B^2\Sigma^+$ state and $v' = 20$ of the $A^2\Pi$ state interacts with the $v = 7$ vibrational level of the $B^2\Sigma^+$ state. These interactions are confirmed from the observed perturbations in the $v' = 9$, 13 and 20 levels of the $A^2\Pi$ state. The effect of interactions is also seen in some lower vibrational levels of the $A^2\Pi$ state. For these levels some spectroscopic constants have abnormal magnitudes and higher order spectroscopic constants are needed to minimize the standard deviation of the fit. The term values for $v' \geq 6$ were given lower weights in the fit for the equilibrium vibrational constants in the $A^2\Pi$ state. We have noticed that the rotational constants of the excited vibrational levels are less affected except for a few levels such as $v' = 9$, 13 and 20. The rotational constants for the affected levels as well as those for the $v' \geq 19$ were given reduced weights in the determination of the equilibrium rotational constants. The equilibrium constants for the two states are provided in Tables 3 and 4. The equilibrium rotational constants obtained from this work are $B_e = 1.6444919(21)$ cm^{-1} for the $A^2\Pi$ state and $B''_e = 1.82084919(48)$ cm^{-1} for the $X^2\Sigma^+$ state which provide the equilibrium bond lengths of 1.23303836(79) Å and 1.17180533(16) Å for the excited and ground states, respectively.

CN is an astrophysical molecule and is observed prominently in carbon stars. The rich CN spectra of carbon stars provide a stringent test for the available CN line list. The CN lines in the 2.0–2.5 μm region were previously used by Lambert et al. [7] for a $^{12}C/^{13}C$ abundance analysis. The complete set of measurements for the $A^2\Pi$–$X^2\Sigma^+$ bands with $v' = 0$–22 for $^{12}C^{14}N$ [21] and those for the same levels of $^{13}C^{14}N$ reported in the present paper will prove useful in astronomical identifications and for a better $^{12}C/^{13}C$ abundance analysis.

5. Summary

The electronic spectra of the $A^2\Pi$–$X^2\Sigma^+$ transition of the $^{13}C^{14}N$ radical have been investigated in the 15000–24000 cm^{-1} region using high resolution spectra recorded with a Fourier transform spectrometer. The spectrum of 27 bands involving vibrational levels up to $v' = 22$ of the excited state and $v'' = 12$ of the ground state has been measured and rotationally analyzed. Our previous measurements of several $A^2\Pi$–$X^2\Sigma^+$ bands with vibrational levels $v' = 0$–8 and $v'' = 0$–5 [23], previous infrared [29,30] and millimeter-wave measurements [31,32] of the ground state have been combined with the present measurements to extract an improved set of spectroscopic constants for the $v' = 0$–22 vibrational levels of the $A^2\Pi$ state of $^{13}C^{14}N$. The new measurements and spectroscopic parameters from this work should prove helpful in interpreting CN spectra seen in comets and stellar atmospheres.

Acknowledgments

The spectra were recorded at the Kitt Peak National Solar Observatory operated by the Association for Research in Astronomy, Inc., under contract with the National Science Foundation. We thank R. Engleman, J. Wagner, C. Plymate and G. Ladd of the National Solar Observatory for assistance in recording and archiving the spectra. The research described here was partially supported by funds from the NASA laboratory astrophysics program. We thank the Leverhulme Trust for financial support through a Research Project Grant.

Appendix A. Supplementary data

Supplementary data for this article are available on ScienceDirect (www.sciencedirect.com) and as part of the Ohio State University Molecular Spectroscopy Archives (http://library.osu.edu/sites/msa/jmsa_hp.htm). Supplementary data associated with this article can be found, in the online version, at http://dx.doi.org/10.1016/j.jms.2012.03.008.

References

[1] K.P. Huber, G. Herzberg, Molecular Spectra and Molecular Structure IV. Constants of Diatomic Molecules, Van Nostrand Reinhold, New York, 1979.
[2] I.R. Ferrin, Astrophys. Space Sci. 52 (1977) 11–16.
[3] N. Fray, Y. Bénilan, H. Cottin, M.-C. Gazeau, J. Crovisier, Planetary Space Sci. 53 (2005) 1243–1262.
[4] J.L. Greenstein, Astrophys. J. 126 (1958) 106–113.
[5] J.R. Johnson, U. Fink, H.P. Larson, Astrophys. J. 270 (1983) 769–777.
[6] A. Fowler, H. Shaw, Roy. Soc. 86A (1912) 118–130.
[7] D.L. Lambert, J.A. Brown, K.H. Hinkle, H.R. Johnson, Astrophys. J. 284 (1984) 223–237.
[8] H. Uitenbroek, A. Tritschler, Astron. Astrophys. 462 (2007) 1157–1163.
[9] A. Wootten, S.M. Lichten, R. Sahai, P.G. Wannier, Astrophys. J. 257 (1912) 151–160.
[10] G.R. Wiedemann, D. Deming, D.E. Jennings, K.H. Hinkle, J.J. Keady, Astrophys. J. 382 (1991) 321–326.
[11] B.E. Turner, R.H. Gammon, Astrophys. J. 198 (1975) 71–89.
[12] D.M. Meyer, M. Jura, Astrophys. J. 297 (1985) 119–132.
[13] R. Riffel, M.G. Pastoriza, A. Rodriguez-Ardila, C. Maraston, Astrophys. J. 659 (2007) L103–L106.
[14] L.M. Hobbs, J.A. Thorburn, T. Oka, J. Barentine, T.P. Snow, D.G. York, Astrophys. J. 615 (2004) 947–957.
[15] M. Wang, C. Henkel, Y.-N. Chin, J.B. Whiteoak, M.H. Cunningham, R. Mauersberger, D. Muders, Astron. Astrophys. 422 (2004) 883–905.
[16] C. Savage, A.J. Apponi, L.M. Ziurys, Astrophys. J. 587 (2002) 211–219.
[17] S.N. Milam, C. Savage, M.A. Brewster, L.M. Ziurys, S. Wyckoff, Astrophys. J. 623 (2005) 1126–1132.
[18] C.V.V. Prasad, P.F. Bernath, J. Mol. Spectrosc. 156 (1992) 327–340.
[19] B.D. Rehfuss, M.-H. Suh, T.A. Miller, V.E. Bondybey, J. Mol. Spectrosc. 151 (1992) 437–458.
[20] C.V.V. Prasad, P.F. Bernath, J. Mol. Spectrosc. 151 (1992) 459–473.
[21] R.S. Ram, L. Wallace, P.F. Bernath, J. Mol. Spectrosc. 263 (2010) 82–88.
[22] R.S. Ram, S.P. Davis, L. Wallace, R. Engleman, D.R.T. Appadoo, P.F. Bernath, J. Mol. Spectrosc. 237 (2006) 225–231.
[23] R.S. Ram, L. Wallace, K. Hinkle, P.F. Bernath, Astrophys. J. Suppl. Ser. 188 (2010) 500–505.
[24] R.S. Ram, P.F. Bernath, Astrophys. J. Suppl. Ser. 194 (2011) 34.
[25] R. Colin, P.F. Bernath, J. Mol. Spectrosc. 273 (2012) 30–33.
[26] T.D. Fay, A.A. Wyller, Solar Phys. 11 (1970) 384–387.
[27] V. Hill, B. Plez, R. Cayrel, T.C. Beers, B. Nordstrom, J. Andersen, M. Spite, F. Spite, B. Barbuy, P. Bonifacio, E. Depagne, P. Francois, F. Primas, Astron. Astrophys. 387 (2002) 560–579.
[28] D.A. Garcia-Hernandez, K.H. Hinkle, D.L. Lambert, K. Eriksson, Astrophys. J. 696 (2009) 1733–1754.
[29] F. Hempel, J. Röpcke, A. Pipa, P.B. Davies, Mol. Phys. 101 (2003) 589–594.
[30] M. Hübner, M. Castillo, P.B. Davies, J. Röpcke, Spectrochim. Acta A 61 (2005) 57–60.
[31] M. Bogey, C. Demuynck, J.L. Destombes, Can. J. Phys. 62 (1984) 1248–1253.
[32] M. Bogey, C. Demuynck, J.L. Destombes, Chem. Phys. 102 (1986) 141–146.
[33] U.G. Jørgensen, M. Larsson, Astron. Astrophys. 238 (1990) 424–434.
[34] D. Shi, H. Liu, X. Zhang, J. Sun, Z. Zhu, Y. Liu, J. Mol. Struct. Theochem. 956 (2010) 10–19.
[35] W. Whaling, W.H.C. Anderson, M.T. Carle, J.W. Brault, H.A. Zarem, J. Res. Natl. Inst. Stand. Technol. 107 (2002) 149–169.
[36] C.J. Sansonetti, J. Res. Natl. Inst. Stand. Technol. 112 (2007) 299–302.
[37] B.R. Vujišić, D.S. Pesić, J. Mol. Spectrosc. 128ć (1988) 334–349.
[38] J.M. Weibberg, E.S. Fishburne, K.N. Rao, J. Mol. Spectrosc. 22 (1967) 406–418.
[39] G. Hosinsky, L. Klynning, B. Lindgren, Phys. Scr. 25 (1982) 291–294.
[40] F.J. LeBlanc, J. Chem. Phys. 48 (1968) 1841–1842.
[41] C. Lonley, J.B. Halpern, J. Wood, C. Vaughn, W.M. Jackson, Chem. Phys. Lett. 73 (1980) 224–227.
[42] N. Furio, A. Ali, P. Dagdigian, J. Mol. Spectrosc. 134 (1989) 199–213.
[43] J.M. Brown, E.A. Colbourn, J.K.G. Watson, F.D. Wayne, J. Mol. Spectrosc. 74 (1979) 294–318.
[44] M. Douay, S.A. Rogers, P.F. Bernath, Mol. Phys. 64 (1988) 425–436.
[45] C. Amiot, J.-P. Maillard, J. Chauville, J. Mol. Spectrosc. 87 (1981) 196–218.